

1 **EXPERIMENTAL GRANULOMATOUS PULMONARY NOCARDIOSIS in**
2 **BALB/c MICE**

3 Short title: GRANULOMATOUS PULMONARY NOCARDIOSIS in MICE

4 Roque M. Mifuji Lira¹, Alberto Yairh Limón Flores¹, Mario César Salinas Carmona¹, Alejandro
5 Ortiz Stern^{1*}.

6 ¹ Departamento de Inmunología, Facultad de Medicina, Universidad Autónoma de Nuevo León,
7 Monterrey, Nuevo León, México.

8 * Corresponding author

9 E-mail: alejandro.ortizst@uanl.edu.mx (AOS)

10

11

12 **Abstract**

13 Pulmonary nocardiosis is a granulomatous disease with high mortality that affects both
14 immunosuppressed and immunocompetent patients. The mechanisms leading to the establishment
15 and progression of the infection are currently unknown. An animal model to study these
16 mechanisms is sorely needed. We report the first *in vivo* model of granulomatous pulmonary
17 nocardiosis that closely resembles human pathology. BALB/c mice infected intranasally with two
18 different doses of GFP-expressing *Nocardia brasiliensis* ATCC700358 (NbGFP), develop weight
19 loss and pulmonary granulomas. Mice infected with 10^9 CFUs progressed towards death within a
20 week while mice infected with 10^8 CFUs died after five to six months. Histological examination of
21 the lungs revealed that both the higher and lower doses of NbGFP induced granulomas with NbGFP
22 clearly identifiable at the center of the lesions. Mice exposed to 10^8 CFUs and subsequently to 10^9
23 CFUs were not protected against disease severity but had less granulomas suggesting some degree
24 of protection. Attempts to identify a cellular target for the infection were unsuccessful but we found
25 that bacterial microcolonies in the suspension used to infect mice were responsible for the
26 establishment of the disease. Small microcolonies of NbGFP, incompatible with nocardial doubling
27 times starting from unicellular organisms, were identified in the lung as early as six hours after
28 infection. Mice infected with highly purified unicellular preparations of NbGFP did not develop
29 granulomas despite showing weight loss. Finally, intranasal delivery of nocardial microcolonies was
30 enough for mice to develop granulomas with minimal weight loss. Taken together these results
31 show that *Nocardia brasiliensis* microcolonies are both necessary and sufficient for the
32 development of granulomatous pulmonary nocardiosis in mice.

33

34 **Introduction**

35 Pulmonary nocardiosis is a serious disease with high mortality [1]. While it usually affects
36 immunocompromised patients there are reports of the disease in apparently normal hosts [2–4].

37 Classical bacteriological studies had shown that most cases of pulmonary nocardiosis were due to
38 *Nocardia asteroides* but advances in genomic taxonomy have shown these to be mostly *N.*
39 *farcinica*, *N. nova* and *N. cyriacigeorgica* [5], while most nocardial infections of the skin are caused
40 by *Nocardia brasiliensis* [6]. Work by Beaman et. al. spanning almost three decades studied
41 nocardial infections in a wide variety of animal hosts using *Nocardia asteroides* and other species
42 of nocardia. Studies with *Nocardia asteroides* showed that mice were able to successfully control
43 pulmonary infection within a week [7], through the coordinated action of IFN γ producing
44 neutrophils [8], recruited via CXCR2 [9], T $\gamma\delta$ cells and IL-17 cells [10]. Additionally, work by
45 Abraham et. al. [11] inoculating *N. brasiliensis* intravenously to mice showed abscess formation in
46 the lungs. No other successful models of pulmonary nocardiosis have been reported, even when
47 rabbit lung macrophages have been successfully infected by nocardia *in vitro* [12]. Pulmonary
48 nocardiosis in humans however, usually presents as a chronic or subacute suppurative disease with
49 formation of granulomas and consolidated areas of the lung [2]. Hence, a proper pulmonary
50 granulomatous nocardiosis model is sorely lacking.

51 Unlike pulmonary nocardiosis, an adequate murine model of actinomycetoma exists. Mice infected
52 with 10^7 CFUs of *Nocardia brasiliensis* in the footpad develop a progressive disease with formation
53 of abscesses and fistulae characteristic of human pathology [13]. Working up from the mycetoma
54 model and through the use of GFP-expressing *Nocardia brasiliensis* (NbGFP) (to facilitate
55 detection) [14] we sought to develop a new model of pulmonary nocardiosis to better study the
56 disease and its immunological aspects. We report the successful development of an experimental
57 pulmonary granulomatous nocardiosis model that should be useful in many settings: to study lung
58 immune responses towards nocardia, to investigate granuloma formation through the use of an
59 infectious agent of minimal virulence to humans and in pre-clinical trials of new anti-nocardial
60 agents.

61

62 **Results**

63 **Intranasal instillation of *Nocardia brasiliensis* leads to pulmonary granulomas**

64 NbGFP isolated from a murine mycetoma and tested for GFP positivity using a photodocumenter
65 set to λ 488 nm was grown for 72 hrs on BHI medium without stirring. After 72 hrs NbGFP formed
66 a biofilm on the surface of the culture media (Sup Fig. 1). Biomass was washed with saline solution
67 and homogenized with a Potter-Elvehjem homogenizer. The bacterial suspension was left to settle
68 and the top half, containing a homogeneous unicellular suspension (as evaluated with a Neubauer
69 chamber) was adjusted to a concentration of 10^{10} CFUs per 50 μ l. Serial 1/10 dilutions were then
70 prepared to infect mice intranasally. These same serial 1/10 dilutions were plated and CFUs were
71 corroborated by colony counting.

72 Based on previous infectious models using *Nocardia spp.* [10] we first tested a dose of 10^6 CFUs
73 without any infected BALB/c mice showing symptoms or signs of disease. In a second experiment
74 mice receiving 10^{10} CFUs died within 24 hours and were not studied any further. Mice were then
75 tested in two independent experiments with doses of 10^9 and 10^8 CFUs. Most mice receiving 10^9
76 CFUs died or had to be sacrificed within a week after losing in average up to 21.5% of their original
77 body weight by day 2 ($p= 6.45E-008$ vs day 0) without showing signs of recovery (Fig 1A and B).
78 On the contrary 80% of mice receiving 10^8 CFUs survived the infection after mild weight loss
79 (8.4% day 2 vs day 0 $p= 0.0001$) that was completely recovered within three weeks (Fig 1A and B).
80 After sacrifice, lungs were excised and filled with a buffered 10% formalin solution. Images of the
81 lungs were captured with a photodocumenter at λ 488 nm and then further processed for
82 histological analysis. Lungs of mice infected with 10^9 CFUs had high numbers of GFP positive dots
83 (Fig 1C) shown to be Kinyoun-positive granules upon histological examination (Fig 1E). Lungs of
84 mice infected with 10^8 CFUs analysed 21 days after infection also had GFP positive dots, albeit at
85 much lower numbers (white arrows in Fig 1D). These lesions appear as granulomas containing
86 Kinyoun-positive nocardia (Fig 1F left panel). Mature granulomas were defined by the clear

87 presence of activated macrophages and lymphocytes surrounding the nocardia (Fig 1F right panel).
88 We decided to follow the long term progression of the disease in two mice infected with low doses
89 of NbGFP. Six months after the infection both mice looked unhealthy and had difficulty moving.
90 Mice were euthanized and lungs processed as previously described. Lungs of these mice had
91 massive abscesses and upon histological examination these were shown to contain a large amount
92 of cellular debris, nocardial microcolonies and severe disruption of surrounding tissue (Fig 1G).

93

94 **Figure 1: Intranasal instillation of *Nocardia brasiliensis* leads to pulmonary granulomas. A)**

95 BALB/c mice received 10^8 (black) or 10^9 (red) NbGFP CFUs and were weighted daily. Individual
96 mice are shown B) Data from A analysed as average \pm s.e.m. The two surviving 10^9

97 CFUs-receiving mice were excluded. C) Lungs from mice receiving 10^9 CFUs were analysed at day
98 4 post infection by whole lung imaging at λ 488 nm. Representative images of two lungs are shown.

99 D) Lungs from mice receiving 10^8 CFUs were analysed at day 21 post infection by whole lung
100 imaging at λ 488 nm. Representative images of two lungs are shown. White arrows point to GFP⁺

101 lesions. E) Representative images of lesions present in mice receiving 10^9 CFUs at day 4 post
102 infection. Kinyoun's stain. Red stained NbGFP is evident at the core of the lesion. F)

103 Representative images of lesions present in mice receiving 10^8 CFUs at day 21 post infection. Left
104 panel: Kinyoun's stain. Red stained NbGFP is evident at the core of the lesion. Right panel: H&E
105 staining. White arrow: NbGFP, black arrows: activated macrophages, black arrowheads:

106 lymphocytes. G) Whole lung imaging and histological (Kinyoun's stain) analysis of a lung from a
107 mice six months after infection with 10^8 NbGFP CFUs. Graphs show data from two independent
108 experiments (n=11 (10^8), 8 (10^9)) * p<0.05 vs. initial weight, ** p<0.01 vs. initial weight, ***

109 p<0.001 vs. initial weight, # p<0.05 10^8 vs. 10^9 , ## p<0.01 10^8 vs. 10^9 , ### p<0.001 10^8 vs. 10^9 .

110

111 **10⁸ dose intranasal infection diminishes granuloma load upon 10⁹ dose challenge.**

112 Even though mice that received 10⁸ CFUs did not completely clear the infection, as evidenced by
113 the presence of granulomas by three weeks and abscesses six months after inoculation, we sought to
114 test if exposure to the lower doses of NbGFP provided protection against a higher dose challenge.
115 Two groups of mice received either saline solution or 10⁸ CFUs NbGFP and 21 days afterwards
116 both groups received 10⁹ CFUs. Both groups lost weight similarly after the second challenge (17.2
117 +/- 4% vs 13.3 +/- 0.09% p=0.52 low dose vs saline, respectively) and surprisingly mice in both
118 groups survived with the exception of a single mouse in the saline receiving group (Fig 2A).
119 However upon examination of the lungs in the photodocumenter, lungs from mice that had received
120 a previous 10⁸ dose of NbGFP had significantly less dots than mice that had received saline solution
121 (Fig 2B and C). We hypothesized that we could have inadvertently given mice a slightly smaller
122 dose than 10⁹ during the second challenge or alternatively that mice in our facility could have had a
123 concomitant non-diagnosed infection that altered the course of the disease. We then repeated the
124 experiment with a new set of SPF mice. Just like in the first experiment, both groups of mice, those
125 that received 10⁸ CFUs and those that received saline solution lost weight similarly upon challenge
126 with 10⁹ CFUs. However disease severity was greater than in previous experiments and all mice had
127 to be sacrificed 4 days after the infection (Fig 2D). Upon analysis of the lungs with the
128 photodocumenter, mice that had been exposed to a lower dose prior to challenge had reduced
129 numbers of granulomas when compared with naive mice exposed to saline solution (Fig 2E and F).
130 Taken together these experiments suggest that severity of the disease during the first days after
131 infection may not be directly related with granuloma burden and that previous exposure to 10⁸
132 CFUs of NbGFP protects mice against developing higher number of lesions upon exposure to 10⁹
133 CFUs.

134 **Figure 2: Low dose intranasal infection diminishes granuloma load upon high dose challenge.**

135 A) BALB/c mice received saline (green) or 10⁸ (blue) NbGFP CFUs and were weighted daily. At

136 day 21 post infection mice were challenged with 10^9 NbGFP CFUs. Weight at day 21 was
137 re-normalized as 100%. B) Lungs from mice challenged with 10^9 CFUs at day 21 were analysed at
138 day 7 post challenge by whole lung imaging at λ 488 nm. Representative images of two lungs per
139 group are shown. C) Average number of lesions per animal from experiment depicted in A and B
140 (n=5 mice per group) D) SPF BALB/c mice received saline (green) or 10^8 (blue) NbGFP CFUs and
141 were weighted daily. At day 21 post infection mice were challenged with 10^9 NbGFP CFUs. Weight
142 at day 21 was re-normalized as 100% E) Lungs from SPF/mice challenged with 10^9 CFUs at day 21
143 were analysed at day 4 post challenge by whole lung imaging at λ 488 nm. Representative images
144 of two lungs per group are shown. F) Average number of lesions per animal from experiment
145 depicted in D and E (n=5 mice per group). Graphs show average +/- s.e.m. (n=5 per group) *
146 $p < 0.05$ vs. initial weight, ** $p < 0.01$ vs. initial weight, *** $p < 0.001$ vs. initial weight, # $p < 0.05$ 10^8
147 vs. 10^9 , ## $p < 0.01$ 10^8 vs. 10^9 , ### $p < 0.001$ 10^8 vs. 10^9 .

148

149 **Heat killed NbGFP causes weight loss upon intranasal delivery**

150 Since granuloma burden and disease severity did not seem to have an absolute correlation, we
151 wanted to know if bacterial components were capable of causing weight loss in BALB/c mice
152 regardless of granuloma formation. Mice exposed to 10^9 heat-killed CFUs lost up to 9.4 % of their
153 body weight one day after inoculation (Sup Fig 2). Image analysis of the lungs of those mice
154 revealed that they did not develop granulomas at any time point (Sup Fig 2).

155

156 **No cell could be identified as a target for NbGFP in the lung**

157 Current models of nocardiosis pose that the macrophage is the prime target for nocardial infections
158 [12,15,16]. In order to test if alveolar macrophages were the target for NbGFP, we isolated
159 macrophages from bronchoalveolar lavages (BAL) of naive mice and exposed them to NbGFP
160 (1:10, Macrophage:NbGFP) for up to 48 hours and imaged the cells every 24 hours. Unlike bone

161 marrow derived macrophages (Fig 3A), alveolar macrophages were not susceptible to infection by
162 NbGFP (Fig 3A). Additionally alveolar macrophages isolated from BAL of inoculated mice were
163 also not infected (Fig 3A). We then hypothesized that it was possible for other phagocytic cells in
164 the airway to be subverted by NbGFP. Given the fact that after inoculation of 10^9 CFUs only some
165 60 lesions are apparent in the lungs of infected mice, such cell should be found in very low
166 numbers. We isolated BAL from infected mice 24 and 48 hours after infection to analyse it by flow
167 cytometry targeting eosinophils as a low prevalence possible target for NbGFP (Fig 3B). BAL
168 analysis showed that eosinophils while present in the lungs of infected animals, did not appear
169 infected (Fig 3B). Flow cytometry showed that most GFP positive cells appeared to be neutrophils,
170 however, by 48 hours the number of GFP+ neutrophils had sharply declined, suggesting addecuate
171 killing of phagocytosed nocardia as reported by Beaman [9]. Additionally, the number of GFP+
172 neutrophils was not compatible with the number of lesions present in the lung 7 days after the
173 infection suggesting that neutrophils are not the target of the infection (Fig 3C).

174 **Figure 3: Neither alveolar macrophages nor eosinophils nor neutrophils are targets for**
175 **NbGFP infection in the lung.** A) Bone marrow derived macrophages (BMDM) or alveolar
176 macrophages (AM) were incubated *in vitro* with NbGFP (1:10) and imaged at 2 hours and at 48 hrs
177 post infection. Cells from BALF of infected mice were imaged 48 hrs after infection to look for
178 infected alveolar macrophages. Representative images are shown. B) BALF analysis of eosinophils
179 by flow cytometry. Left panel shows non-specific events detected within the eosinophil gate in the
180 absence of CCR3 staining. Right panel shows no increase in GFP+ events amongst eosinophils
181 stained with an anti-CCR3 antibody. C) BALF analysis of granulocytes by flow cytometry at 24
182 (left panel) and 48 (right panel) hours post infection.

183

184 **Microscopic bacterial microcolonies are responsible for the formation of granulomas**

185 We then turned to confocal microscopy to try to identify cells that could harness large numbers of

186 bacteria at early time points. Analysis of lungs at 6 hrs, and 24 hrs after infection did not reveal the
187 presence of spots detectable with the photodocumenter while granulomas were clearly present at 7
188 days (Fig 4A). Microscopic confocal analysis of lung sections from mice infected with 10^9 CFUs
189 NbGFP at 6 and 24 hours after infection revealed the presence of microscopic microcolonies of
190 NbGFP surrounded by inflammatory cells (Fig 4B), but no microcolonies were found inside cells of
191 any kind. Growth curves for NbGFP suggest a doubling time of 7.8 hours (Fig 4C), which is
192 incompatible with the presence of bacterial microcolonies at such early time points. Infection with
193 wild type *Nocardia brasiliensis* (ATCC700358) also produced granulomas when instilled
194 intranasally (Sup Fig.3).

195 **Figure 4: NbGFP microcolonies are present in the lungs of infected mice as early as 6 hours**
196 **post infection.** A) Lungs from mice receiving 10^9 CFUs were analysed at 6 hours, 1 day and 4 days
197 post infection by whole lung imaging at λ 488 nm. Representative images of two lungs per time
198 point are shown. B) Confocal microscopy images of lung sections at 6 and 24 hours post infection.
199 C) Growth curve of NbGFP under constant stirring to prevent biofilm formation.

200

201 To test if bacterial microcolonies were responsible for granuloma formation we removed NbGFP
202 microcolonies from the suspension prior to intranasal instillation. Mice that received a highly
203 purified unicellular 10^9 CFUs dose, lost almost as much weight as mice receiving a regular 10^9
204 CFUs suspension, however none of the mice developed lesions 4 days after inoculation while mice
205 that received the regular suspension developed granulomas (Fig 5A, B and E). Finally we isolated
206 bacterial microcolonies and prepared a suspension that was examined visually to contain between
207 50 to 100 microcolonies per 50 μ l. Mice infected with this suspension lost very little weight which
208 they recovered at day 2. Upon both image and microscopic analysis these mice were shown to have
209 nocardial lesions by day 4 (Fig 5D and F). Mice infected with bacterial microcolonies and analysed
210 21 days after infection also had lesions corresponding to mature granulomas as evidenced by the

211 presence of activated macrophages and lymphocytes surrounding the nocardia (Fig 5G).

212 **Figure 5: Microscopic bacterial microcolonies are responsible for the formation of**

213 **granulomas.** A) BALB/c mice (n=3 per group) received 10^9 (red) or 10^9 Highly purified single-cell (purple)

214 NbGFP CFUs and were weighted daily. B) Lungs from mice in A were analysed at day 4 post

215 infection by whole lung imaging at λ 488 nm. Representative images of two lungs per group are

216 shown. C) BALB/c mice (n=5 per group) received 10^9 (red) CFUs or ≈ 100 (teal) NbGFP

217 microcolonies and were weighted daily. D) Lungs from mice in D were analysed at day 4 post

218 infection by whole lung imaging at λ 488 nm. Representative images of two lungs per group are

219 shown. White arrows point to GFP⁺ lesions. E) Representative histology of lungs in mice receiving

220 10^9 Highly purified single-cell CFUs at day 4 post infection. Kinyoun's stain. F) Representative images of

221 lesions present in mice receiving microcolonies. Kinyoun's stain. Red stained NbGFP is evident at

222 the core of the lesion. G) Representative H&E image of lesions present in mice 21 days after

223 infection with purified microcolonies. White arrows: NbGFP, black arrows: activated macrophages,

224 black arrowheads: lymphocytes.

225 **Inflammation drives lethality of infection with 10^9 CFUs**

226 While nocardial microcolonies drive the formation of granulomas, the mechanism for the lethality

227 seen when infecting mice with 10^9 CFUs was not clear. The acute weight loss observed in these

228 mice point towards an exacerbated inflammatory response. To evaluate the inflammatory response

229 we analysed BAL cell numbers, protein content and IL-1 β levels of mice infected with either 10^8 or

230 10^9 CFUs 24 and 48 hours after infection (Sup Fig. 4). BAL cell numbers at 24 hours post infection

231 were not different between the 10^9 or 10^8 dose. However, the amount of GFP⁺ neutrophils was, by

232 far, larger on animals infected with the higher dose. At 48 hours post-infection BAL cell numbers

233 and neutrophil content was clearly diminishing on mice receiving 10^8 CFUs. In clear contrast, BAL

234 cell numbers and total neutrophils increased between 24 and 48 hours in mice given 10^9 CFUs.

235 Additionally, the number of GFP⁺ neutrophils remained elevated (Sup Fig. 4B-F). BAL protein

236 levels were significantly elevated only in mice receiving 10^9 CFUs both at 24 and 48 hours post
237 infection (Sup Fig. 4G). IL-1 β levels were eight fold higher in mice receiving 10^9 CFUs ($148.9 \pm$
238 21.5 pg/ml) compared with mice receiving 10^8 CFUs (18.3 ± 5.6 pg/ml) 24 hours post infection.
239 Furthermore, IL-1 β remained elevated at 48 hours post infection in mice receiving 10^9 CFUs (100.3
240 ± 13.02 pg/ml) while they became undetectable in mice receiving 10^8 CFUs (Sup Fig. 4H).

241

242 Taken together these results provide very strong evidence that microscopic bacterial microcolonies
243 are both necessary and sufficient for *Nocardia brasiliensis* to cause granulomatous pulmonary
244 nocardiosis in mice.

245

246 **Discussion**

247 To our knowledge this is the first description of an animal model of pulmonary granulomatous
248 nocardiosis. While work by Beaman and collaborators has helped to understand some of the
249 immune responses towards nocardial infections, much has been missed by the fact that animals
250 infected intranasally with *Nocardia asteroides* do not develop granulomatous disease [10]. Previous
251 work by Abraham and collaborators showed that mice receiving intravenous *N. brasiliensis*
252 developed lung abscesses containing the pathogen but not granulomas. This discrepancy with our
253 results could be explained by the various methodological differences, namely, the route of
254 administration, bacterial load, bacterial strain and the use of steroids [11].

255 In pursuing the goal of developing a granulomatous model we departed from the methodology used
256 by Beaman [17]. The main difference, apart from our use of *Nocardia brasiliensis*, is that our
257 inoculum is derived from a disrupted biofilm instead of a culture grown in agitation. While this
258 methodology, the disruption of *N. brasiliensis* biofilms, had been reported to produce single
259 organisms [13] we found that disruption is not complete and microcolonies remain in bacterial

260 suspensions prepared this way. These microcolonies were not easily identified when our first set of
261 experiments were performed, the most likely explanation as to why we did not detect them could be
262 the high dilution needed to adjust CFUs for infection which precluded their detection (Sup Fig. 1).
263 Thus the inoculum used to infect mice in our first experiments was a mixture of single-celled
264 organisms and bacterial microcolonies. Mice infected with this preparation still presented a
265 dose/response relationship; mice infected with higher CFUs evolved with worst clinical outcomes
266 and more granulomas. Both our experiments to test for protection and those aimed at identifying the
267 target cell of the infection were carried out under the idea that single cell organisms were
268 responsible for the infection.

269 The finding that alveolar macrophages were not susceptible to *Nocardia brasiliensis* infection
270 neither *in vitro* nor *in vivo* was very unexpected in the light of current knowledge of nocardial
271 diseases [15] and prompted us to look for alternatives. Analysis of lungs at very early time points
272 after infection were crucial to understanding the pathogenesis of the disease since presence of
273 microcolonies as early as six hours post infection were completely incompatible with single-cell
274 organisms being responsible due to nocardial doubling times of 8 hours. It will be important to
275 understand the role of alveolar macrophages within the context of nocardial granulomas to see if
276 their organization is comparable to that of other granulomatous diseases (i.e. tuberculosis) where
277 pro-inflammatory macrophages lie mostly at the center and anti-inflammatory macrophages reside
278 in the periphery of the granuloma [18]. Analysis of mice that received 10^8 CFUs of the unfiltered
279 NbGFP or purified microcolonies 21 days after the infection revealed that the lesions seen at 4 days
280 indeed progress towards the formation of a mature granuloma with activated macrophages and
281 lymphocytes surrounding the nocardia. Studying the phenotype of these cells should yield rich
282 results regarding granuloma formation and progression.

283 It is interesting to notice that granulomas generated in the lung in response to *N. brasiliensis*
284 nocardial microcolonies very much resemble the lesions seen in subcutaneous actinomycetomas.

285 While working on this manuscript we conducted an extensive image search looking for
286 histopathological samples of human pulmonary nocardiosis due to *Nocardia brasiliensis* to
287 directly compare with our findings but we were unsuccessful, none seem to be documented.
288 However, one report of an invasive *N. brasiliensis* infection of the skin with pulmonary
289 involvement showed lesions extremely similar to the ones we show in this manuscript [19].
290 Additionally, granulomas due to other *Nocardia spp.* present themselves with a similar architecture
291 to the lesions we describe in this manuscript, namely, extracellular bacteria surrounded by
292 macrophages and lymphocytes [20]. The importance of granulomas in pulmonary nocardiosis is
293 further underscored by the fact that pulmonary nodules are the second most common radiographic
294 finding in pulmonary nocardiosis [21]. Furthermore in a report of endobronchial nocardiosis masses
295 of nocardia, very much like our microcolonies were seen upon biopsy of the lesions [22].
296 Our experiments with highly purified single-cell organisms and microcolonies further clarified their
297 role in the disease. Single-cell organisms, accounting for most of the 10^8 - 10^9 CFUs given to mice,
298 appear responsible for the acute inflammatory response and weight loss seen upon infection. On the
299 contrary, microcolonies did not cause such weight loss. While it could be possible to speculate that
300 single-cell organisms could cause granulomas after longer time periods, we think this is unlikely,
301 given that upon microscopic examination, no granulomatous or pre-granulomatous lesion could be
302 seen four days after infection, a time at which colonies are already apparent to the naked eye upon
303 culture in agar plates.
304 Our studies on protection suggested that weight loss was mostly due to an inflammatory response.
305 Mice infected with 10^8 CFUs and then re-challenged with 10^9 CFUs lost as much weight as mice
306 receiving saline and then a challenge with 10^9 CFUs. When addressed directly it became clear that
307 the inflammatory response to 10^9 CFUs was of a grave magnitude comprising intense neutrophil
308 recruitment, augmented protein leakage and high levels of IL1- β . Despite this inflammatory
309 response, a role for immunological memory seems to be present in pre-challenged mice as

310 evidenced by the reduced granuloma burden upon re-challenged. We are currently working in our
311 lab to clarify the nature of this protection.

312 A current view of bacterial pathogenicity suggests that subversion of phagocytes is highly related
313 with low infectious doses [23]. However this view assumes that single organisms, or multiple
314 individual organisms, are responsible for infections. Our data adds one more possibility, the ability
315 to grow as microcolonies or to dislodge as microcolonies from biofilms. While biofilm formation
316 has been largely explored as a problem on medical devices and other surfaces [24] the study of its
317 role in other infectious routes has just started. microcolonies as infectious units of the airways
318 should be limited by size, large microcolonies ($>15 \mu\text{m}$) would be unable to travel past the upper
319 airways and microcolonies smaller than macrophages ($< 8\mu\text{m}$) should be effectively managed by
320 professional phagocytes [25]. We are currently working towards pinpointing precisely the minimal
321 microcolony size required for progression to granuloma as this will allow us to study granuloma
322 formation and progression in both early and late phases of the disease.

323 In conclusion, *Nocardia brasiliensis* microcolonies are sufficient and necessary to cause
324 granulomatous pulmonary nocardiosis in immunocompetent BALB/c mice. Additionally, this
325 experimental model should be useful in helping to understand granulomatous diseases, through the
326 use of an infectious agent of minimal virulence to humans, and in pre-clinical trials of new
327 anti-nocardial agents.

328

329 **Materials and Methods**

330 **Ethics Statement**

331 All experimental protocols and care of the animals were approved by the Comité Institucional para
332 el Cuidado y Uso de Animales de Laboratorio (CICUAL) within the Ethics Committee of the
333 Facultad de Medicina, Universidad Autónoma de Nuevo León. The protocol registration with the

334 CICUAL Ethics Committee is: IN 13-005. The Ethics Committee, recognized by the National
335 Bioethics Commission (CONBIOETICA19CEI00320130404) and the Secretaría de Salud via
336 COFEPRIS (13CEI1903937), operates under national guidelines for the use, care and handling of
337 laboratory animals as established by the Norma Oficial Mexicana (NOM-062-ZOO-1999).
338 Anesthesia was provided for all procedures involving animals using a Ketamine/Xylazine mixture.

339 **Inoculum preparation and growth analysis**

340 *Nocardia brasiliensis* (ATCC 700 358) expressing green fluorescent protein (NbGFP) [14], was
341 cultured in 50 ml BHI broth (Brain Heart Infusion, Oxoid, Hampshire, England) supplemented with
342 gentamycin sulfate (Garamicina®, Schering-Plough S.A., Mexico) 26 µg/ml for 72 hours at 37° C
343 without stirring. Biofilms from three Erlenmeyer flasks were resuspended in sterile saline and
344 homogenized using a Potter-Elvehjem homogenizer to obtain a unicellular suspension. Suspensions
345 were allowed to settle for 10 minutes and the top phase was recovered, centrifuged, weighted and
346 resuspended to 250 mg/ml (which yields 10¹⁰ CFUs per 50 µl as corroborated by serial dilution
347 plating in at least five independent experiments). From there different doses of colony-forming units
348 (CFUs) were prepared through dilutions, corroborated using a Neubauer chamber and by serial
349 dilution plating. For growth analysis NbGFP was grown under constant stirring and optical density
350 sampled at λ 600nm (SmartSpec Plus, Bio-Rad Laboratories) at shown intervals. Nocardial
351 doubling times were calculated to be 7 hours and 28 minutes using exponential regression. Highly
352 purified single-cell NbGFP inoculum was prepared by passing the nocardial suspension through a 4
353 µm pore filter. microcolonies were recovered from the filters and diluted to the desired
354 concentration.

355 **Animals**

356 Mice were housed at the animal facility of the Department of Immunology of the Facultad de
357 Medicina, UANL under controlled temperature, humidity and lighting and *ad libitum* feeding. Male

358 6 to 8 weeks old, BALB/c and SPF BALB/c mice were anesthetized with an intraperitoneal
359 injection of 200 μ l of ketamine (Anesket®, PISA Agropecuaria, Mexico)/xylazine (Procin®, PISA
360 Agropecuaria, Mexico) mixture, containing 2 mg and 0.4 mg respectively. Mice were infected with
361 different doses of NbGFP via intranasal instillation (from 10^6 to 10^{10} CFUs/mouse.) For the immune
362 protection experiments, mice were instilled intranasally with sterile saline or NbGFP 10^8 CFUs and
363 21 days later they were re-challenged with 10^9 CFUs.

364 **Necropsy**

365 Mice were sacrificed via cervical dislocation. Lungs were excised, filled with, and submerged in a
366 buffered 10% formalin solution.

367 **Macroscopic analysis**

368 Inflated lungs were analysed with a photodocumenter (ChemiDoc™ MP System, Bio-Rad
369 Laboratories), at λ 488nm. Images were analysed and adjusted for brightness and contrast using
370 ImageJ. Lesions were manually scored by 2 independent researchers.

371 **Microscopic analysis**

372 Inflated and fixed lungs in buffered 10% formalin solution for 48 hrs were cut and dehydrated in
373 70% ethanol for 2 hours, 80% ethanol 1 hour, 95% ethanol 1 hour, and 3 changes of 100% ethanol
374 for 1 hour. After tissue dehydration, lungs were transferred to xylene (Xileno RA, CTR Scientific,
375 Mexico) 3 changes of 1.5 hours each. Lungs were then submerged in 60° C paraffin (Paraplast®
376 regular, Sigma-Aldrich, MO, U.S.A.) twice, for 2 hours, and embedded in individual cassettes. 5
377 μ m lung sections were deparaffinized using 1.7% dishwashing soap solution as described by Amita
378 Negi [26], and dyed using Kinyoun's stain (Carbol fuchsin, Sigma-Aldrich, MO, U.S.A., and
379 Methylene Blue, Sigma-Aldrich, MO, U.S.A). Images were acquired using Carl Zeiss Axio Scope
380 A1 equipped with AxioCam ERc 5s and imaging software AxioVision v. 4.8. For confocal
381 microscopy, lung sections were deparaffinized and mounted in media with

382 4',6-diamidino-2-phenylindole (DAPI) (VECTASHIELD® with DAPI, Vector laboratories, CA,
383 U.S.A). Images were acquired using Carl Zeiss LSM 710-NLO Multiphoton Confocal Microscope
384 equipped with imaging software ZEN (Zeiss efficient navigation) version 5.5.0.0.

385 **Bronchoalveolar lavage**

386 Bronchoalveolar lavage fluid was obtained from naive or NbGFP infected mice (one or two days
387 after infection) by 3x 1 ml washes with warm saline. Alveolar macrophages from naive mice were
388 allowed to adhere to plastic culture plates for 6 hours before infection with NbGFP as described
389 below for BMDM. Alveolar macrophages from infected mice were incubated for 48 hrs and imaged
390 as described for BMDM.

391 **Flow Cytometry**

392 BAL cells from infected mice were incubated with 1/500 dilutions of A647-antiCCR3 (clone
393 J073E5, Biolegend), PE-Gr1 (clone RB6-8C5, Biolegend) for 30 minutes at room temperature and
394 washed 3x in 10 volumes of 0.5% BSA PBS. Cells were processed using a LSRFortessa
395 (BDBiosciences) equipped with Diva software. Analysis and figure preparation was performed with
396 Flowing Software 2 (<http://www.flowingsoftware.com/>)

397 **NbGFP in vitro infection**

398 We obtained bone marrow derived macrophages (BMDM) by culturing bone marrow cells obtained
399 from femur and tibia from BALB/c mice in RPMI with 30% L929-Conditioned Medium (LCM) as
400 described by Weischenfeldt J, [27]. BMDM were co-cultured with NbGFP at MOI 1:10 for 48 hours
401 in 6 well plates. Images were obtained and analysed using Life technologies, FLoid® Cell Imaging
402 Station.

403 **Statistical analysis**

404 Intra-group and inter-group differences were compared by paired and unpaired two-tailed T-tests

405 respectively. $p < 0.05$ was considered significant. Statistical analysis was performed using Microsoft
406 Excel.

407

408 **Acknowledgements**

409 We are thankful for the excellent technical assistance provided by Alejandra Gallegos Velasco.

410 Confocal microscopy was carried out under the technical supervision of Juan Carlos Segoviano

411 Ramírez at Unidad de Bioimagen, Centro de Investigación y Desarrollo en Ciencias de la Salud

412 (CIDICS), Universidad Autónoma de Nuevo León, Nuevo León, México.

413 **References**

414 1. Baracco GJ, Dickinson GM. Pulmonary Nocardiosis. *Curr Infect Dis Rep.* 2001;3: 286–292.

415

416 2. Menéndez R, Cordero PJ, Santos M, Gobernado M, Marco V. Pulmonary infection with
417 *Nocardia* species: a report of 10 cases and review. *Eur Respir J.* 1997;10: 1542–1546.

418

419 3. Martínez R, Reyes S, Menéndez R. Pulmonary nocardiosis: risk factors, clinical features,
420 diagnosis and prognosis. *Curr Opin Pulm Med.* 2008;14: 219–227.

421 doi:10.1097/MCP.0b013e3282f85dd3

422

423 4. Dominguez DC, Antony SJ. Actinomyces and nocardia infections in immunocompromised and
424 nonimmunocompromised patients. *J Natl Med Assoc.* 1999;91: 35–39.

425

426 5. Brown-Elliott BA, Conville P, Wallace Jr. RJ. Current Status of *Nocardia* Taxonomy and
427 Recommended Identification Methods. *Clin Microbiol Newsl.* 2015;37: 25–32.

428 doi:10.1016/j.clinmicnews.2015.01.007

429

430 6. Minero MV, Marín M, Cercenado E, Rabadán PM, Bouza E, Muñoz P. Nocardiosis at the Turn
431 of the Century: *Medicine (Baltimore).* 2009;88: 250–261. doi:10.1097/MD.0b013e3181afa1c8

432

433 7. Beaman BL, Goldstein E, Gershwin ME, Maslan S, Lippert W. Lung response to congenitally
434 athymic (nude), heterozygous, and Swiss Webster mice to aerogenic and intranasal infection by
435 *Nocardia asteroides*. *Infect Immun.* 1978;22: 867–877.

436

- 437 8. Ellis TN, Beaman BL. Murine polymorphonuclear neutrophils produce interferon- γ in response
438 to pulmonary infection with *Nocardia asteroides*. *J Leukoc Biol.* 2002;72: 373–381.
439
- 440 9. Moore TA, Newstead MW, Strieter RM, Mehrad B, Beaman BL, Standiford TJ. Bacterial
441 clearance and survival are dependent on CXC chemokine receptor-2 ligands in a murine model
442 of pulmonary *Nocardia asteroides* infection. *J Immunol Baltim Md 1950.* 2000;164: 908–915.
443
- 444 10. Tam S, Maksareekul S, Hyde DM, Godinez I, Beaman BL. IL-17 and $\gamma\delta$ T-lymphocytes play a
445 critical role in innate immunity against *Nocardia asteroides* GUH-2. *Microbes Infect Inst*
446 *Pasteur.* 2012;14: 1133–1143. doi:10.1016/j.micinf.2012.05.008
447
- 448 11. Mishra SK, Sandhu RS, Randhawa HS, Damodaran VN, Abraham S. Effect of Cortisone
449 Administration on Experimental Nocardiosis. *Infect Immun.* 1973;7: 123–129.
450
- 451 12. Beaman BL. In vitro response of rabbit alveolar macrophages to infection with *Nocardia*
452 *asteroides*. *Infect Immun.* 1977;15: 925–937.
453
- 454 13. Salinas-Carmona MC, Torres-Lopez E, Ramos AI, Licon-Trillo A, Gonzalez-Spencer D.
455 Immune Response to *Nocardia brasiliensis* Antigens in an Experimental Model of
456 Actinomycetoma in BALB/c Mice. *Infect Immun.* 1999;67: 2428–2432.
457
- 458 14. Salinas-Carmona MC, Rocha-Pizaña MR. Construction of a *Nocardia brasiliensis* fluorescent
459 plasmid to study Actinomycetoma pathogenicity. *Plasmid.* 2011;65: 25–31.
460 doi:10.1016/j.plasmid.2010.09.005
461
- 462 15. Silva CL, Faccioli LH. Tumor necrosis factor and macrophage activation are important in
463 clearance of *Nocardia brasiliensis* from the livers and spleens of mice. *Infect Immun.* 1992;60:
464 3566–3570.
465
- 466 16. Trevino-Villarreal JH, Vera-Cabrera L, Valero-Guillen PL, Salinas-Carmona MC. *Nocardia*
467 *brasiliensis* Cell Wall Lipids Modulate Macrophage and Dendritic Responses That Favor
468 Development of Experimental Actinomycetoma in BALB/c Mice. *Infect Immun.* 2012;80:
469 3587–3601. doi:10.1128/IAI.00446-12
470
- 471 17. Tam S, King DP, Beaman BL. Increase of $\gamma\delta$ T Lymphocytes in Murine Lungs Occurs during
472 Recovery from Pulmonary Infection by *Nocardia asteroides*. *Infect Immun.* 2001;69:
473 6165–6171. doi:10.1128/IAI.69.10.6165-6171.2001
474
- 475 18. Mattila JT, Ojo OO, Kepka-Lenhart D, Marino S, Kim JH, Eum SY, et al. Microenvironments in
476 Tuberculous Granulomas Are Delineated by Distinct Populations of Macrophage Subsets and
477 Expression of Nitric Oxide Synthase and Arginase Isoforms. *J Immunol.* 2013;191: 773–784.
478 doi:10.4049/jimmunol.1300113

479

480 19. Zehra Y, Murat A, Hilal O, Mehmet AÖ, Neslihan F, Fahrettin T, and Erdoğan Ç. An Unusual
481 Case of Pulmonary Nocardiosis in Immunocompetent Patient. Case Reports in Pulmonology.
482 2014. doi:10.1155/2014/963482

483 19. Muñoz-Hernández B, Noyola MC, Palma-Cortés G, Rosete DP, Galván MA, Manjarrez
484 MEActinomycetoma in arm disseminated to lung with grains of *Nocardia brasiliensis* with
485 peripheral filamentsMycopathologia. 2009 Jul;168(1):37-40. doi: 10.1007/s11046-009-9189-5.
486 Epub 2009 Feb 24.

487 21. Hui CH, Au VW, Rowland K, Slavotinek JP, Gordon DL. Pulmonary nocardiosis re-visited:
488 experience of 35 patients at diagnosis. Respir Med. 2003 Jun;97(6):709-17.
489 doi:10.1053/rmed.2003.1505

490 22. Cakir E, Buyukpinarbasili N, Ziyade S, Selcuk-Duru HN, Bilgin M, Topuz U. Endobronchial
491 nocardiosis in an 11-year-old child. Pediatr Pulmonol. 2013 Nov;48(11):1144-7. doi:
492 10.1002/ppul.22740. Epub 2012 Dec 31.

493 23. Gama JA, Abby SS, Vieira-Silva S, Dionisio F, Rocha EPC. Immune Subversion and
494 Quorum-Sensing Shape the Variation in Infectious Dose among Bacterial Pathogens. PLoS
495 Pathog. 2012;8: e1002503. doi:10.1371/journal.ppat.1002503

496 24. Mihai MM, Holban AM, Giurcăneanu C, Popa LG, Oanea RM, Lazăr V, et al. Microbial
497 Biofilms: Impact On Pathogenesis Of Periodontitis, Cystic Fibrosis, Chronic Wounds And
498 Medical Device-Related Infections. Curr Top Med Chem. 2015;
499

500 25. Byron PR. Prediction of drug residence times in regions of the human respiratory tract
501 following aerosol inhalation. J Pharm Sci. 1986;75: 433–438. doi:10.1002/jps.2600750502
502

503 26. Negi A, Puri A, Gupta R, Chauhan I, Nangia R, Sachdeva A. Biosafe alternative to xylene: A
504 comparative study. J Oral Maxillofac Pathol JOMFP. 2013;17: 363–366.
505 doi:10.4103/0973-029X.125199
506

507 27. Weischenfeldt J, Porse B. Bone Marrow-Derived Macrophages (BMM): Isolation and
508 Applications. CSH Protoc. 2008;2008: pdb.prot5080.
509

510 Supporting Information Captions

511 **Sup Fig 1. Isolation, growth and delivery of GFP+ *Nocardia brasiliensis*.**

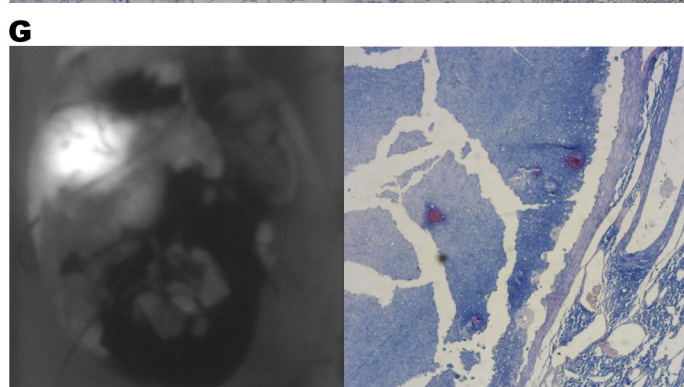
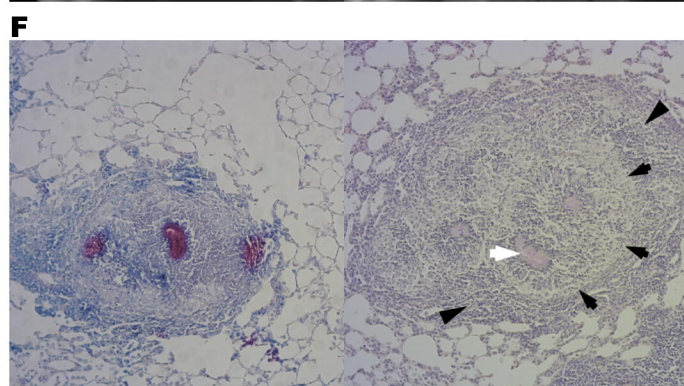
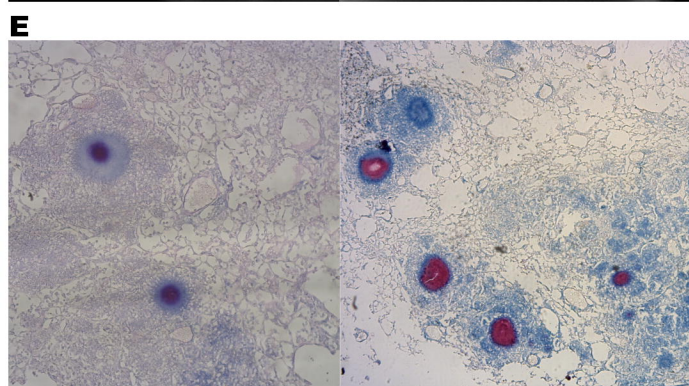
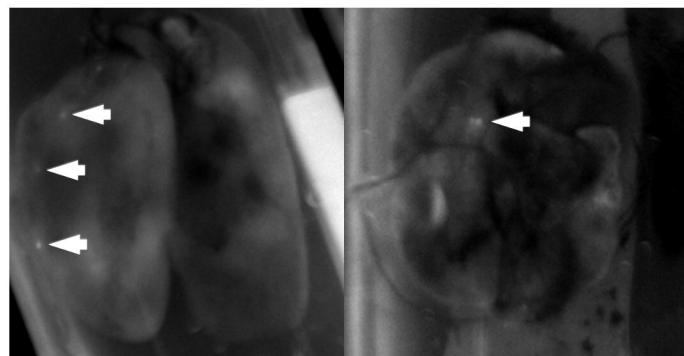
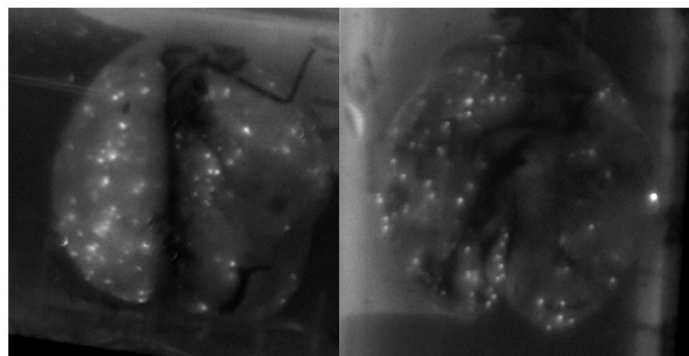
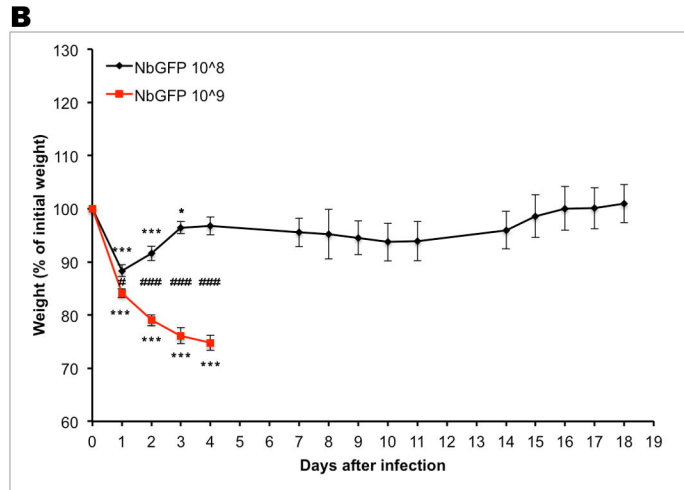
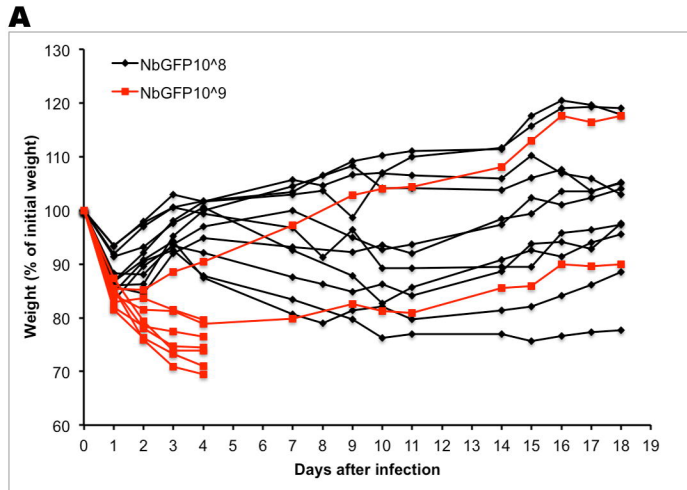
512 **Sup Fig 2. Heat killed NbGFP causes weight loss but not granulomas**

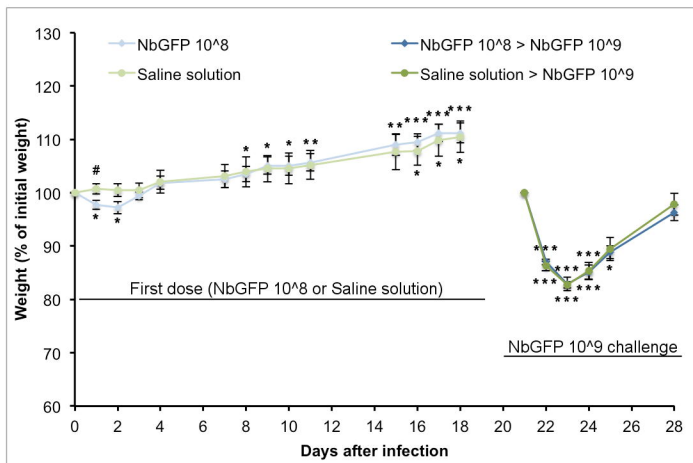
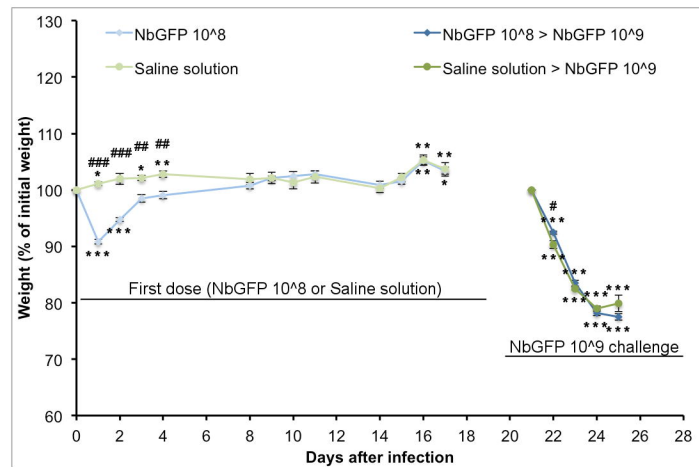
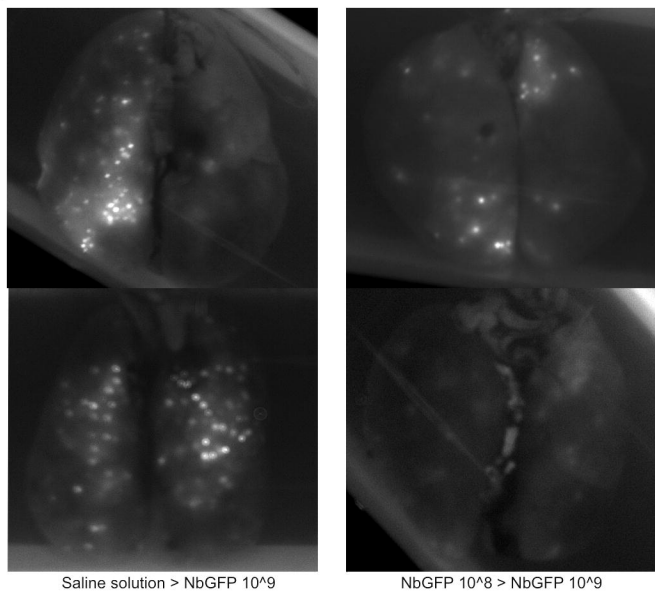
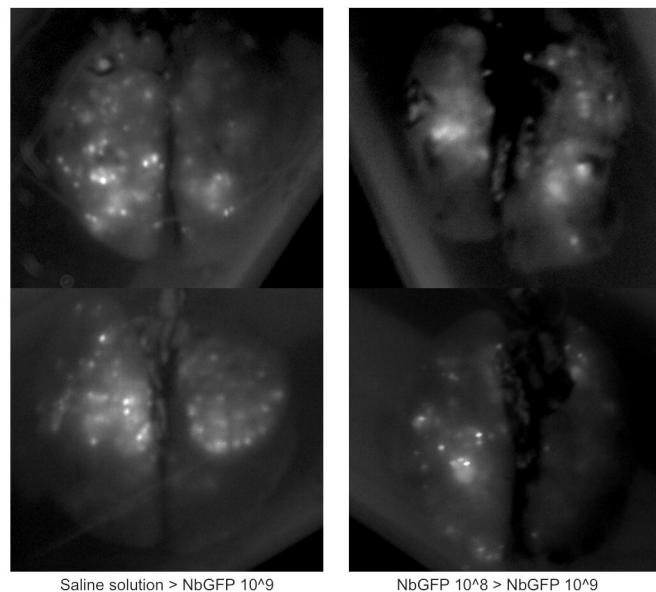
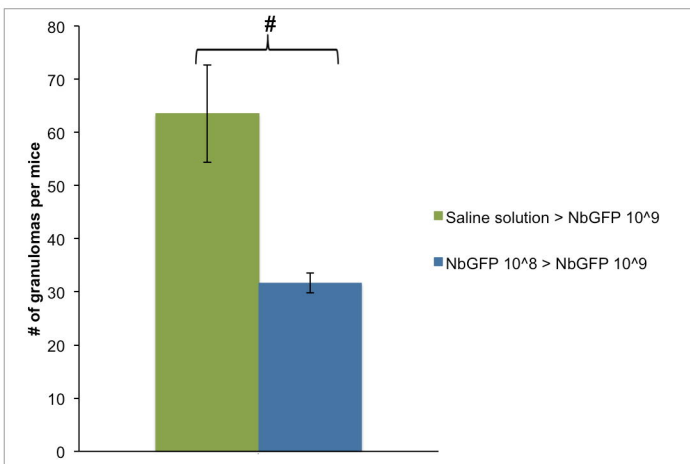
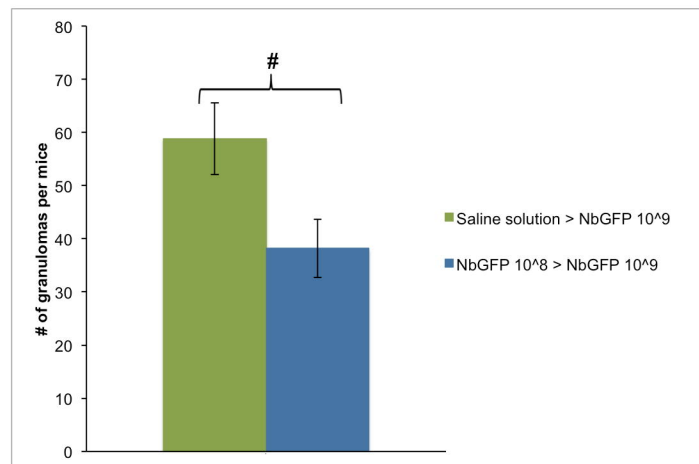
513 **Sup Fig 3. Granuloma due to wild type *N. brasiliensis***

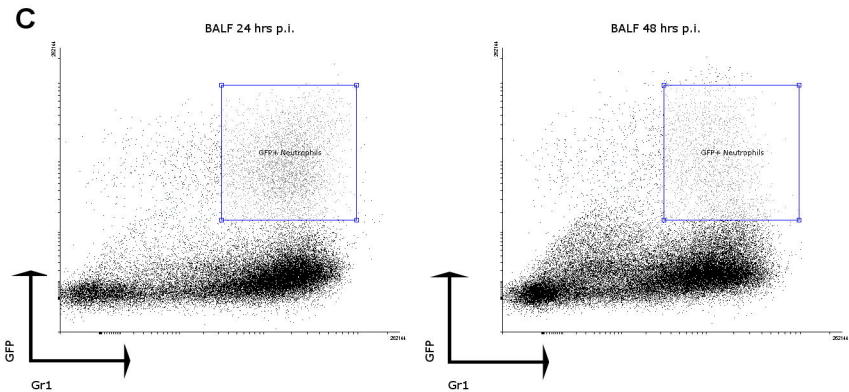
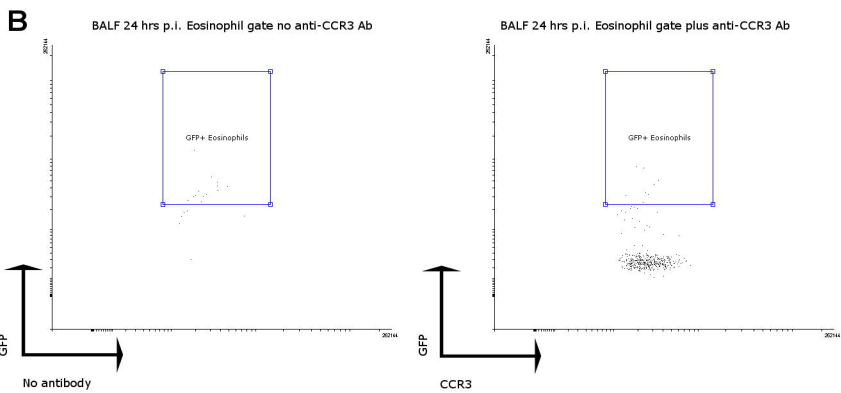
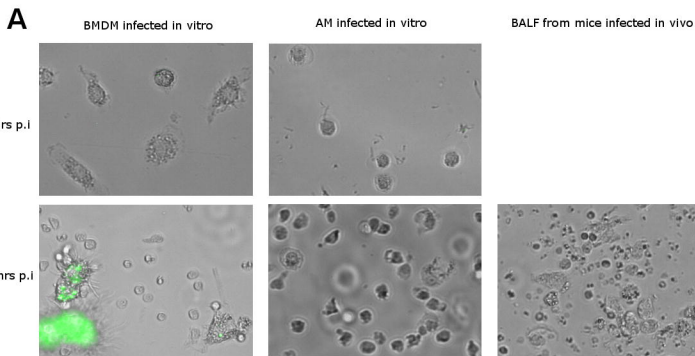
514 **Sup Fig 4. Inflammatory lung response in mice receiving either 10⁸ or 10⁹ NbGFP+ CFUs.**

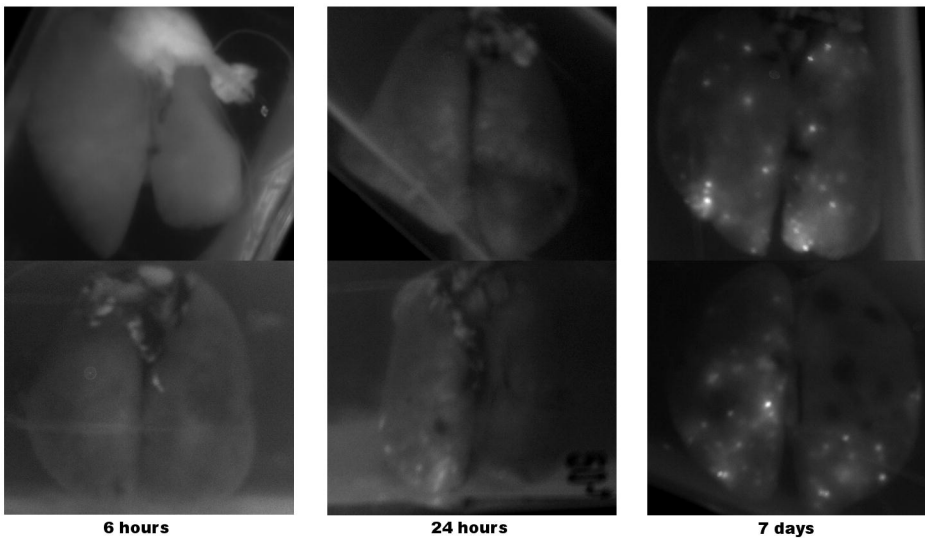
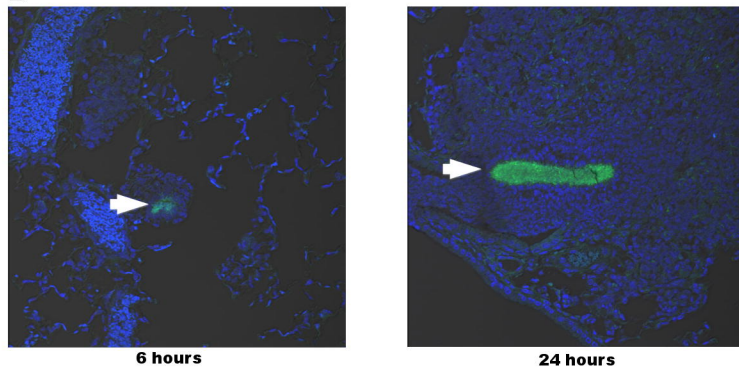
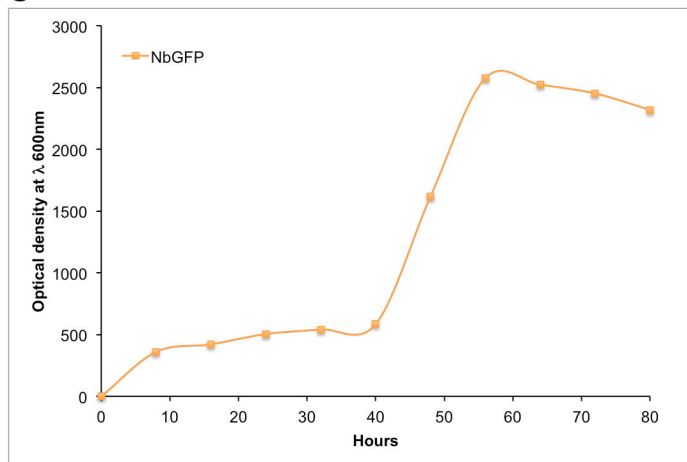
515 Graphs show average +/- s.e.m. (n=5 per group) * p<0.05, ** p<0.01, *** p<0.001, ### p<0.001

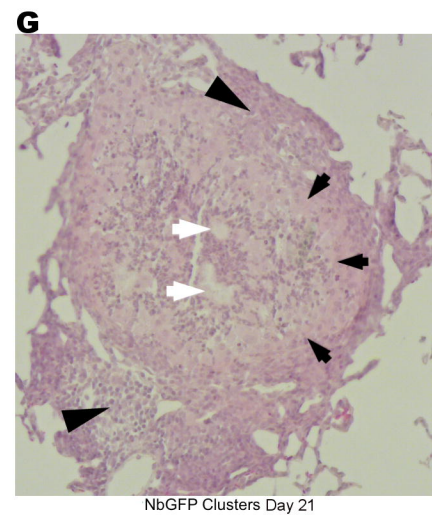
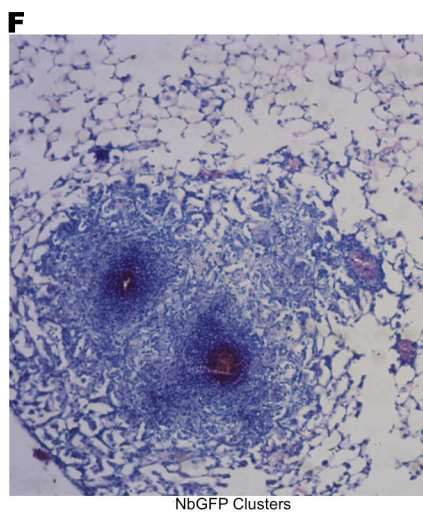
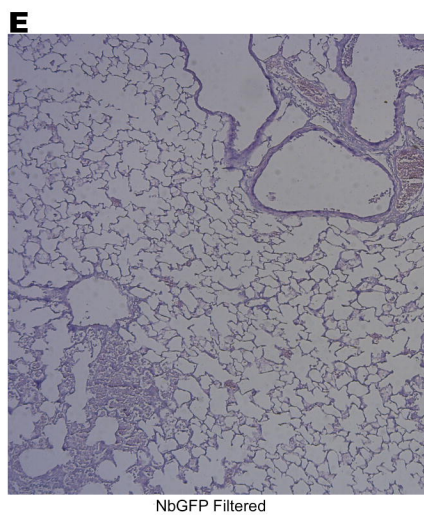
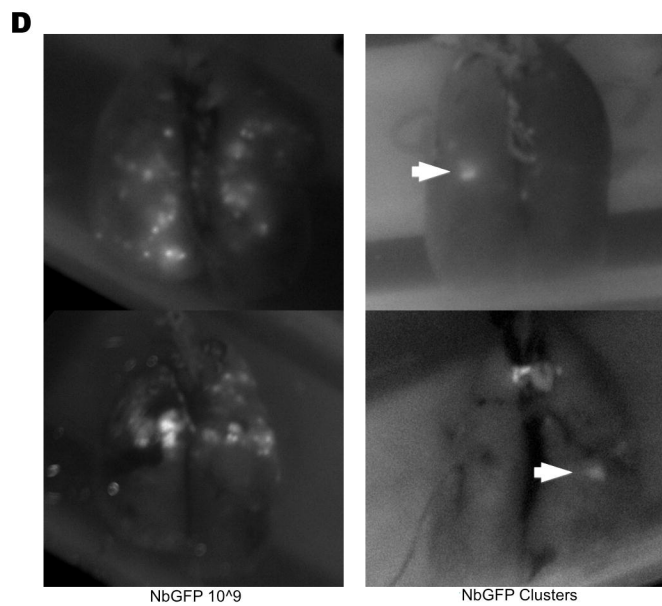
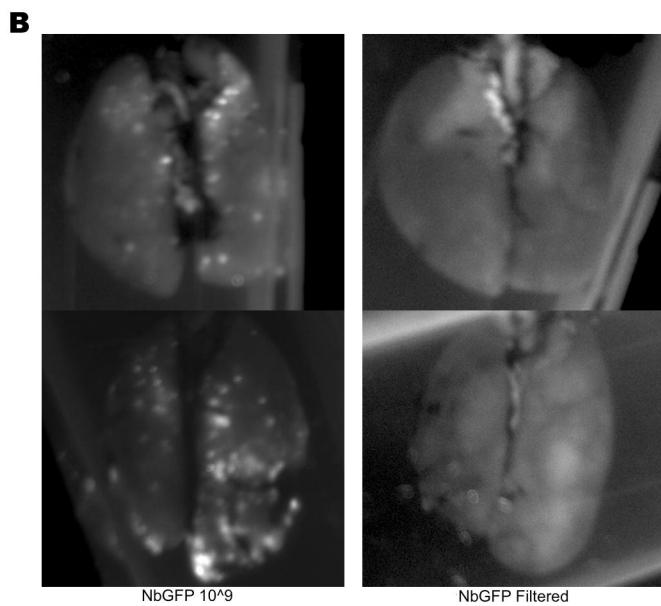
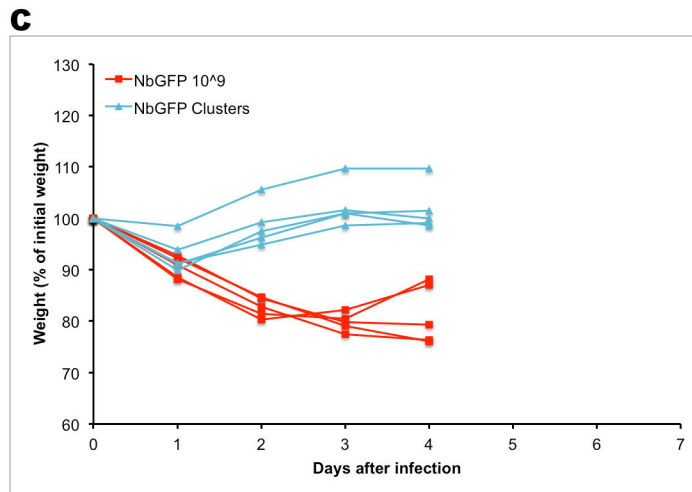
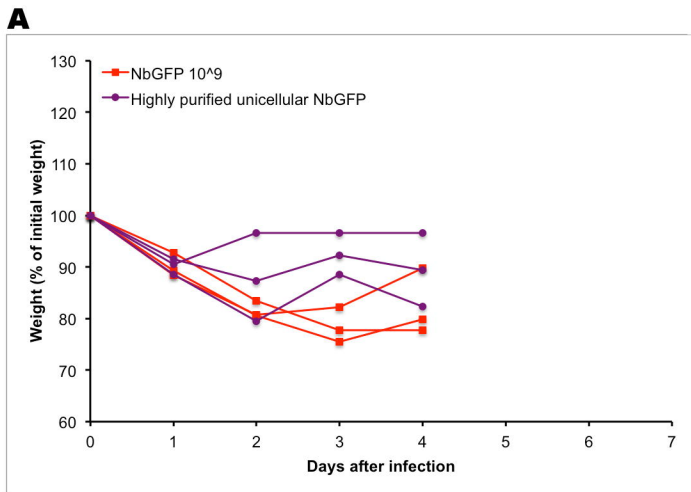
516 10^8 vs. 10^9 , n.d.=not detectable.



A**D****B****E****C****F**

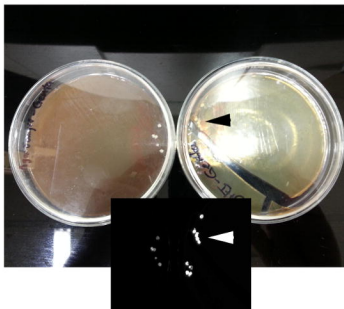


A**6 hours****24 hours****7 days****B****6 hours****24 hours****C**

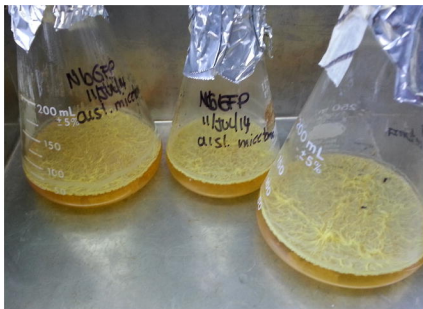




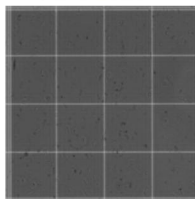
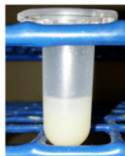
Colonies were isolated from a 30-day old NbGFP+ mycetoma



Single colonies were tested to ensure expression of GFP



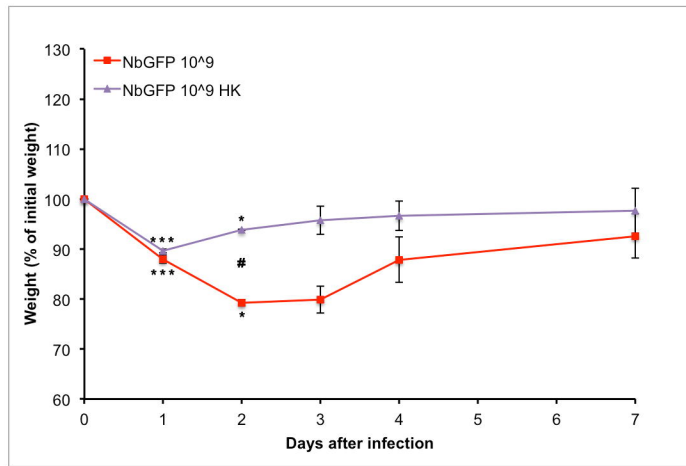
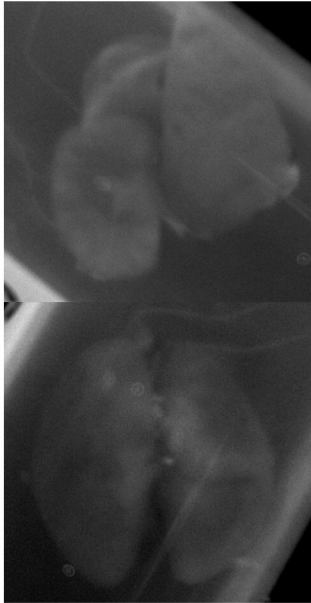
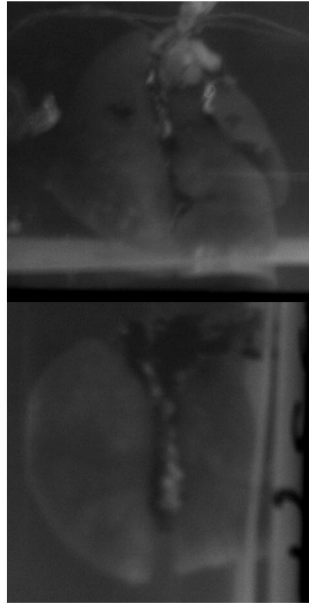
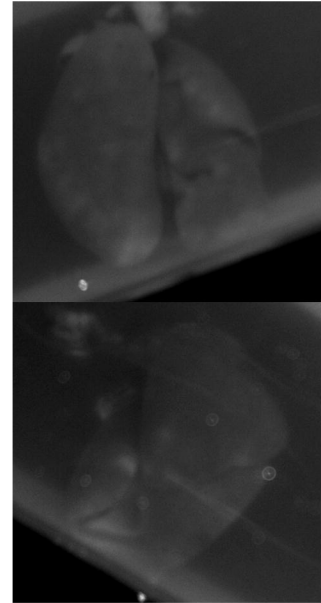
GFP+ *Nocardia brasiliensis* was grown for 72 hrs on BHI



Biofilms were disrupted with a Potter-Elvehjem homogenizer



50 ul of selected bacterial suspensions were delivered i.n.

A**B****6 hours****24 hours****7 days**

